Thermochemistry of N−N Containing Ions: A Threshold Photoelectron Photoion Coincidence Spectroscopy Study of Ionized Methyl- and Tetramethylhydrazine

Anne-Marie Boulanger,[†] Emma E. Rennie,[†,§] David M. P. Holland,[‡] David A. Shaw,[‡] and Paul M. Mayer*[,‡]

Chemistry Department, University of Ottawa, Ottawa, Ontario K1N 6N5 Canada, and Daresbury Laboratory, Daresbury, Warrington, Cheshire WA4 4AD U.K.

Received: September 17, 2007; In Final Form: October 29, 2007

The unimolecular dissociation reactions of the methylhydrazine (MH) and tetramethylhydrazine (TMH) radical cations have been investigated using tandem mass spectrometry and threshold photoelectron photoion coincidence spectroscopy in the photon energy ranges 9.60−31.95 eV (for the MH ion) and 7.74−29.94 eV (for the TMH ion). Methylhydrazine ions ($CH_3NHNH_2^{+\bullet}$) have three low-energy dissociation channels: hydrogen atom loss to form $CH_2NHNH_2^+$ (*m*/*z* 45), loss of a methyl radical to form $NHNH_2^+$ (*m*/*z* 31), and loss of methane to form the fragment ion *m*/*z* 30, $N_2H_2^{+\bullet}$. Tetramethylhydrazine ions only exhibit two dissociation reactions near threshold: that of methyl radical loss to form $(CH_3)_2NNCH_3^+$ (*m*/*z* 73) and of methane loss to form the fragment ion *m*/*z* 72 with the empirical formula $C_3H_8N_2^{+\bullet}$. The experimental breakdown curves were modeled with Rice−Ramsperger−Kassel−Marcus theory, and it was found that, particularly for methyl radical loss, variational transition state theory was needed to obtain satisfactory fits to the data. The 0 K enthalpies of formation ($\Delta_f H_0$) for all fragment ions (*m*/*z* 73, *m*/*z* 72, *m*/*z* 45, *m*/*z* 31, and *m*/*z* 30) have been determined from the 0 K activation energies (E_0) obtained from the fitting procedure: $\Delta_f H_0[(CH_3)_2NNCH_3^+] = 833 \pm 5$ kJ mol^{-1}, $\Delta_f H_0$ $[C_3H_8N_2^{+\bullet}] = 1064 \pm 5$ kJ mol^{-1}, $\Delta_f H_0[CH_2NHNH_2^+] = 862 \pm 5$ kJ mol^{-1}, $\Delta_f H_0[NHNH_2^+] = 959 \pm 5$ kJ mol^{-1}, and $\Delta_f H_0[N_2H_2^{+\bullet}] = 1155 \pm 5$ kJ mol^{-1}. The breakdown curves have been measured from threshold up to $h\nu \approx 32$ eV for both hydrazine ions. As the photon energy increases, other dissociation products are observed and their appearance energies are reported.

Introduction

Cations containing two nitrogen atoms in their backbone have been the subject of only a few experimental and theoretical studies.[1−4] Most of the investigations, carried out in the 1970s, concerned the photoelectron spectroscopy of the azo compounds ($R_1N{=}NR_2$) and some hydrazine derivatives ($R_1R_2N{-}NR_3R_4$).[5−7] The properties of the azo and hydrazine compounds depend on the nature of the substituent R groups. The azo dyes have been traditionally extremely important to industry due to their high stability and to their electronic transitions that occur in the visible region. When R is a relatively stable alkyl radical, the azo dyes become thermally labile and constitute an important class of polymerization initiators. The practical properties of these azo and hydrazine compounds rest mainly on their electronic structure and thermochemistry. That being said, there is a dearth of information on the thermochemistry of N_2 containing free radicals and cations.

Hydrazine and five methyl-substituted hydrazine derivatives were studied almost 50 years ago by Dibeler et al.[8] using electron ionization (EI) mass spectrometry. They reported the appearance energies (AEs) and ionic enthalpies of formation ($\Delta_f H$) of the observed fragment ions. Their reported $\Delta_f H$ were calculated from the AEs of the fragment ions and from $\Delta_f H$ reported by Harshman[9] for the neutral molecules hydrazine, methylhydrazine, 1,1- and 1,2-dimethylhydrazine. However, the enthalpies of formation for trimethylhydrazine and tetramethylhydrazine were estimated using the group equivalents method[10] and were subsequently found to be erroneous.[11]

Between 1989 and 1994, three papers[1,3,4] were published on $CH_5N_2^+$ ions. In the first, Burgers et al.[1] studied the $CH_5N_2^+$ hydrazyl radicals and cations by mass spectrometry. Four distinct singly charged $CH_5N_2^+$ ions were generated from three different molecular ions, and the $\Delta_f H$ of the $CH_5N_2^+$ cations were determined from their measured AEs. As will be seen later, their $\Delta_f H$ values are lower by 50−100 kJ mol^{-1} than those presently determined. In 1992, the group[4] reinvestigated some aspects of the CH_5N_2 potential energy surface based on their previous experimental results[1] and concluded that the reported AEs for the methyl losses from methylhydrazine, 1,1- and 1,2-dimethylhydrazine were not reliable because of interferences from traces of amines. New enthalpies of formation of the $CH_5N_2^+$ fragment ions were also reported as well as proton affinities (PA) for HNNH, $CH_3N{=}NH$, and $CH_3N{=}NCH_3$. Two years later, Nguyen[3] investigated hydrogen cyanide loss from $CH_5N_2^+$ cations using ab initio molecular orbitals calculations. He also reported enthalpies of formation for the $CH_5N_2^+$ ions along with PA values for diazene and methyldiazene. Recently a book[12] on assigning structures to gas-phase ions was published containing some thermochemistry for $CH_5N_2^+$ (*m*/*z* 45) and $C_3H_8N_2^{+\bullet}$ (*m*/*z* 72) fragment ions. No reported structures were available for fragment ions $C_3H_9N_2^+$ (*m*/*z* 73).

Most of the previously reported $\Delta_f H$ for NN-containing ions were determined from measurements of onset AEs for the fragment ions. However, when extracting meaningful thermo-

* Corresponding author. E-mail: pmmayer@uottawa.ca.
† University of Ottawa.
‡ Daresbury Laboratory.
§ Present address: Production Testing, Varian, Inc. 2700 Mitchell Drive, Walnut Creek, CA 94598. Tel: 925-945-2302. E-mail: emma.rennie@varianinc.com.

10.1021/jp077475y CCC: $40.75
Published on Web 01/16/2008

chemical information from AE determinations there are a number of potential problems. First, any rearrangement reaction usually has at least one energetic barrier associated with a transition state that can cause the AE to be higher than the true thermochemical threshold (i.e., there is a reverse energy barrier in the reaction). Second, competitive and kinetic shifts can affect the AEs.[13] Third, if the AE measurements were performed using electrons with a broad energy distribution, the true onset can be difficult to determine. As will be shown in the present study, the $\Delta_f H$ values previously determined from AE measurements for a variety of NN-containing ions are found to be inaccurate.

The present work is part of a larger investigation of NN-containing ions. We have previously studied three methyl-substituted hydrazine compounds (methylhydrazine (MH), 1,1-dimethylhydrazine (UDMH), and tetramethylhydrazine (TMH)), using high-resolution threshold and conventional photoelectron spectrocospy in the photon energy range of 7−32 eV.[11,14] In that study, we were able to measure the adiabatic and vertical ionization energies of all three hydrazine compounds and gain some insight into the inner valence molecular orbitals. Enthalpies of formation of the neutral and ionic hydrazine derivatives were also obtained from ab initio calculations. We then carried out a threshold photoelectron photoion coincidence spectroscopy (TPEPICO) study on 1,1-dimethylhydrazine ions[15] to measure the breakdown curves as a function of photon energy and ion residence time in the threshold region. $\Delta_f H$ values were determined for its two lowest energy fragment ions: $CH_3N{=}NH_2^+$ (m/z 45) and $(CH_3)(CH_2)NNH_2^+$ (m/z 59). The effects of the entropy of activation ($\Delta S^{\ddagger}$) on both unimolecular dissociations of the UDMH ions were investigated by modeling the experimental breakdown curves using a simple form of variational transition state theory (VTST). We now present TPEPICO studies on methylhydrazine and tetramethylhydrazine ions. The breakdown curves of both hydrazine ions were modeled using the simplified form of VTST that we employed previously for 1,1-dimethylhydrazine ions. $\Delta_f H$s for a series of NN-containing ions are derived from experiment and calculated at the modified G3 level of theory: $N_2H_2^{+\bullet}$ m/z 30, $NHNH_2^+$ m/z 31, $CH_2{-}NHNH_2^+$ m/z 45, $C_3H_8N_2^{+\bullet}$ m/z 72, and $(CH_3)_2NNCH_3^+$ m/z 73. These values allow us to explore methyl substitution effects on NN-containing ion $\Delta_f H$ as well as to determine the proton affinities of several NN-containing neutral molecules.

Experimental Procedures

Experimental Overview. The TPEPICO experiments have been carried out at the Daresbury Laboratory synchrotron radiation source. The TPEPICO spectrometer,[16] the 5 m normal incidence monochromator,[17] and the experimental procedures[18] have been described in detail previously.

A pulsed extraction technique allowed the breakdown curve to be recorded as a function of parent ion residence time in the interaction region by changing the time between the detection of the threshold electron and the application of the ion drawout field.[16,18] The residence time is defined as the period between the creation of the electron-ion pair and the application of the pulse and is given by the transit time of the electron added to the electronic signal processing time. The minimum residence time in the current apparatus has been measured as 1.116 ± 0.050 μs using the experimental procedure described in Holland et al.[16] The breakdown curve of methylhydrazine in the first crossover region (between h$\nu \approx$ 9.64 and 11.04 eV) has been measured for four ion residence times, t_{res} = 1.116, 3.116, 5.116, and 7.116 μs, while the breakdown curve of tetramethylhydrazine in the first crossover region (between h$\nu \approx$ 8.62 and 11.02 eV) has been measured for three ion residence times, t_{res} = 1.116, 3.116, and 5.116 μs. The electron transmission function used in the convolution of the calculated breakdown curves was derived from a threshold electron spectrum obtained from the photoionization of krypton in the region of the $^2P_{1/2}$ ionization limit under the conditions used in the TPEPICO measurements.[16]

The mass-analyzed ion kinetic energy (MIKE) and collision-induced dissociation (CID) experiments were performed on a modified VG ZAB mass spectrometer[19] incorporating a magnetic sector followed by two electrostatic sectors (BEE geometry). Ions were generated in the ion source by electron ionization. The pressure inside the ion source was kept at $\sim 1.0 \times 10^{-5}$ Torr as measured with an ionization gauge located above the ion source diffusion pump. CID experiments were performed using helium as the target gas. The helium pressure in the collision cell was approximately 8.0×10^{-8} to 1.0×10^{-7} Torr corresponding to a beam reduction of 10%. Deuterium exchange experiments were done with D_2O. The glass capillary inlet was flushed four times with 10 μL of deuterium oxide prior to the introduction of methylhydrazine. A peak with m/z 49 was observed corresponding to the deuterated methylhydrazine ion ($CH_3NDND_2^{+\bullet}$). Kinetic energy release (KER) measurements were made in the usual manner.[13]

Materials. Methylhydrazine, tetramethylhydrazine (Aldrich, > 97%), and deuterium oxide (MSD Isotopes, 99.9% D) were used without further purification for the MIKE, CID, and KER experiments. For the TPEPICO experiments, the samples were subjected to three freeze-pump-thaw cycles to remove air.

Computational Procedures. Ab initio molecular orbital calculations were performed using the Gaussian 98[20] suite of programs. The methylhydrazine and tetramethylhydrazine ions and all their fragment ions and neutrals were optimized at the B3-LYP/6-31+G(d) level of theory in accordance with a previous assessment carried out for 1,1-dimethylhydrazine ions.[15] A modified G3 (mG3) protocol[21,22] based on the optimized B3-LYP/6-31+G(d) geometries and scaled B3-LYP ZPE (scaling factor = 0.9806) was used to calculate the enthalpies of formation of all (fragment) ions and neutrals. The mG3 energies are found in Table 1.

Potential energy curves were calculated at the B3-LYP/6-31+G(d) level of theory for each simple bond cleavage reaction following the procedure outlined previously for ionized 1,1-dimethylhydrazine.[15] Briefly, each potential energy curve was generated by optimizing the geometry of the dissociating ion at incrementally increasing bond lengths (in 0.1 Å steps) until the energy reached a plateau at the separated products. For example, for the hydrogen loss channel from the methylhydrazine ions the dissociating complex ion structures were optimized from the equilibrium bond length at R_{C-H} = 1.097 Å up to R_{C-H} = 2.597 Å. The vibrational frequencies and the rotational constants were calculated at each step.

The effective transition state at a given internal energy was located by finding the molecular configuration along the potential energy curve that gave the minimum rovibrational sum-of-states ($N^{\ddagger}$).[15,23] As there are obvious limitations in the above approach, it was used only to locate the transition states. The vibrational frequencies of these molecular configurations were used as adjustable parameters to obtain a fit to the experimental breakdown curves according to the procedure outlined previously.[15] The variational $k(E_{int})$ vs E_{int} were convoluted with the electron transmission function, the monochromator bandpass, and the thermal population distribution of the neutral methylhydrazine or tetramethylhydrazine molecule. The sets of rate constants were constructed by combining the rate constants

TABLE 1: Absolute and Relative Energies[a] of the Fragment Ions and Neutrals of the Methylhydrazine and Tetramethylhydrazine Ions at the B3-LYP/6-31+G(d) and mG3[b] Levels of Theory

	absolute energies (hartrees)		relative energies (eV)		relative energies (kJ mol^{-1})	
structures[c]	B3-LYP/6-31+G(d)	mG3	B3-LYP/6-31+G(d)	mG3	B3-LYP/6-31+G(d)	mG3
$CH_3NHNH_2^{+\bullet}$	−150.8266743	−150.7565816	0.000	0.000	0	0
$CH_2NHNH_2^+ + H^\bullet$	−150.7362703	−150.6742534	2.460	2.240	237	216
$CH_2NNH_3^+ + H^\bullet$	−150.7287432	−150.6672078	2.665	2.432	257	235
$CH_3NNH_2^+ + H^\bullet$	−150.7223496	−150.6562740	2.839	2.730	274	263
$CH_3NHNH^+ + H^\bullet$	−150.7173799	−150.6551809	2.974	2.759	287	266
$NHNH_2^+ + CH_3^\bullet$	−150.7188970	−150.6569799	2.933	2.710	283	262
$N_2H_2^{+\bullet}$(trans) + CH_4	−150.7409085	−150.6724733	2.334	2.289	225	221
$N_2H_2^{+\bullet}$(iso) + CH_4	−150.7388647	−150.6687910	2.389	2.389	231	230
$N_2H_2^{+\bullet}$(cis) + CH_4	−150.7308069	−150.6633196	2.609	2.538	252	245
$N_2H_2^{+\bullet}$(trans) + $CH_3^\bullet + H^\bullet$	−150.5780558	−150.5096770	6.765	6.719	653	648
$N_2H_2^{+\bullet}$(iso) + $CH_3^\bullet + H^\bullet$	−150.5760120	−150.5059947	6.821	6.819	658	658
$N_2H_2^{+\bullet}$(cis) + $CH_3^\bullet + H^\bullet$	−150.5679542	−150.5005233	7.040	6.968	679	672
$(CH_3)_2NN(CH_3)_2^{+\bullet}$	−268.7000736	−268.5731606	0.000	0.000	0	0
$(CH_3)_2NNCH_3^+ + CH_3^\bullet$	−268.6352819[d]	−268.5085848[d]	1.763[d]	1.757[d]	170[d]	170[d]
	−268.6352030[e]	−268.5085199[e]	1.765[e]	1.759[e]	170[e]	170[e]
$C_3H_8N_2^{+\bullet}$ isomer I + CH_4	−268.6571618[d]	−268.5254477[d]	1.168[d]	1.298[d]	113[d]	125[d]
	−268.6572195[e]	−268.5255170[e]	1.166[e]	1.296[e]	113[e]	125[e]
$C_3H_8N_2^{+\bullet}$ isomer II + CH_4	−268.6591778	−268.5268281	1.113	1.261	107	122
$C_3H_8N_2^{+\bullet}$ isomer III + CH_4	−268.6713717	−268.5367966	0.781	0.990	75	95
$C_3H_8N_2^{+\bullet}$ isomer IV + CH_4	−268.6713037	−268.5417432	0.783	0.855	76	82
$C_3H_8N_2^{+\bullet}$ isomer V + CH_4	−268.6822996	−268.5465742	0.484	0.723	47	70
$C_3H_8N_2^{+\bullet}$ isomer VI + CH_4	−268.6359898	−268.5028961	1.744	1.912	168	184
$C_3H_8N_2^{+\bullet}$ isomer VII + CH_4	−268.6382087	−268.5042794	1.683	1.874	162	181
$C_3H_8N_2^{+\bullet}$ isomer VIII + CH_4	−268.7030893	−268.5768428	−0.082	−0.100	−8	−10
$C_3H_8N_2^{+\bullet}$ isomer IX + CH_4	−268.6739672	−268.5451725	0.710	0.762	69	73

[a] The absolute and relative energies have been corrected for ZPE (scaling factor = 0.9806). [b] Modified G3 protocol based on optimized B3-LYP/6-31+G(d) geometries and scaled B3-LYP ZPE.[21,22] [c] The methylhydrazine ion, $CH_3NHNH_2^{+\bullet}$, its fragment ion $CH_2NHNH_2^+$, the tetramethylhydrazine ion, $(CH_3)_2NN(CH_3)_2^{+\bullet}$, the trimethylhydrazyl fragment ion $(CH_3)_2NNCH_3^+$, and $C_3H_8N_2^{+\bullet}$ isomers (I to VIII) belong to the C_1 point group. Fragment ions $CH_2NNH_3^+$, $CH_3NNH_2^+$, CH_3NHNH^+, $HNNH_2^+$, and $C_3H_8N_2^{+\bullet}$ isomer IX belong to the C_s point group. Cis-diazene and iso-diazene belong to the C_{2v} point group. Trans-diazene belongs to the C_{2h} point group. The methyl radical belongs to the D_{3h} point group and methane belongs to the T_d point group. The trimethylhydrazyl fragment ion $(CH_3)_2NNCH_3^+$ and $C_3H_8N_2^{+\bullet}$ isomer I fragment ion can also belong to the C_s point group. [d] Energy when fragment ion belongs to the C_1 point group. [e] Energy when fragment ion belongs to the C_s point group.

corresponding to each transition state (for example, see Supporting Information, Table S1 from Boulanger et al.)[15]

For the rearrangement channels involving methane loss, no potential energy curve was calculated. The transition state properties were estimated using the vibrational frequencies of the methylhydrazine or tetramethylhydrazine ion. The vibrational mode corresponding to the C−N stretch was removed and the five lowest vibrational frequencies were scaled until a good fit was obtained to the experimental curve for *m*/*z* 30 (for the MH ion) or *m*/*z* 72 (for the TMH ion). To fit the experimental *m*/*z* 72 breakdown curves for the tetramethylhydrazine ion, a set of two estimated transition states was used. More will be said about this in Results and Discussion.

The rovibrational entropy of activation, $\Delta S^{\ddagger}_{rovib}$, was determined for all dissociation channels according to the East and Radom[24] procedure for the computation of third-law entropies. In their free rotor model, the internal moment of inertia was estimated to be between 3.0−3.1 amu Å^2.[24] In the case of the hydrogen loss channel from the methylhydrazine ion, the hydrogen atom comes from the methyl group. Therefore, the system was treated as having no free rotors in the transition states. For the methane loss channel from methylhydrazine ion, the transition state was treated as having no free rotor while for the same channel from tetramethylhydrazine ion, the transition states were treated as having only two free methyl rotors.

Results and Discussion

Reaction Mechanisms. The MIKE mass spectrum of ionized methylhydrazine exhibits one peak with *m*/*z* 45 corresponding to loss of a hydrogen atom. The CID mass spectrum of this metastably generated *m*/*z* 45 ion is distinct from that of the $CH_3NNH_2^+$ ion generated by methyl loss from metastable 1,1-dimethylhydrazine ions[15] (Figure 1a,b). The doubly charged ion and fragment ion at *m*/*z* 31 are not observed in the CID mass spectrum of the latter ion. $CH_3NDND_2^{+\bullet}$ and $(CH_3)_2NND_2^{+\bullet}$, generated by deuterium exchange experiments on methylhydrazine and 1,1-dimethylhydrazine, gave different fragment ions in their MIKE mass spectra (eqs 1 and 2), indicating that the

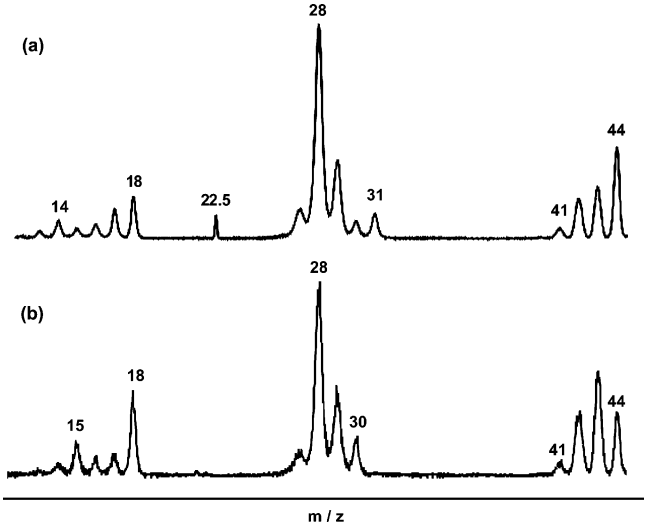

Figure 1. Portions of the CID mass spectra of (a) metastable fragment ion *m*/*z* 45, $CH_2NHNH_2^+$, from the methylhydrazine ion and (b) metastable fragment ion *m*/*z* 45, $CH_3NNH_2^+$, from the 1,1-dimethylhydrazine ion.

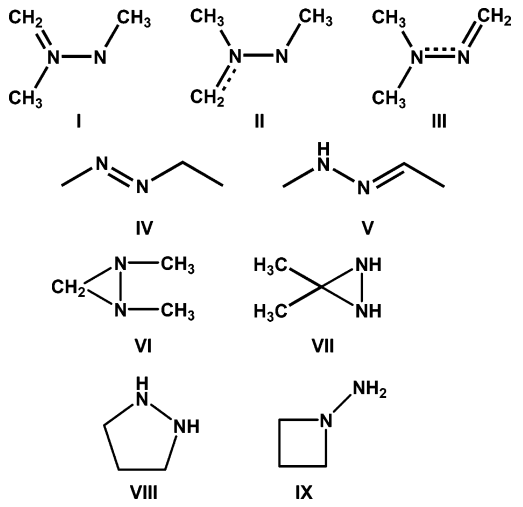

Figure 2. Nine possible isomers of fragment ion *m*/*z* 72 with the empirical formula $C_3H_8N_2^{+\bullet}$.

structures of the two nonlabeled fragment ions with *m*/*z* 45 ($CH_5N_2^+$) are different:

$$CH_3N\mathbf{D}N\mathbf{D}_2^{+\bullet}\ (m/z\ 49) \rightarrow CH_2\mathbf{D}_3N_2^+\ (m/z\ 48) + H^\bullet \quad (1)$$

$$(CH_3)_2NN\mathbf{D}_2^{+\bullet}\ (m/z\ 62) \rightarrow CH_3\mathbf{D}_2N_2^+\ (m/z\ 47) + CH_3^\bullet \quad (2)$$

There are six possible isomers of the $CH_5N_2^+$ fragment ion:[12] $CH_2NHNH_2^+$, $CH_2NNH_3^+$, $CH_3NNH_2^+$, CH_3NHNH^+, cy-$C(H_2)N(H)N(H_2)$-$^+$, and $[HNC{-}NH_4]^+$. The isotopic labeling shows that the hydrogen atom is lost from the methyl group of ionized methylhydrazine to form the $CH_2NHNH_2^+$ fragment ion in agreement with earlier work on the formation of this isomer.[1,4] Calculations at the B3-LYP/6-31+G(d) level of theory and with the modified G3 protocol indicate that the formation of $CH_2NHNH_2^+$ is also the most energetically favorable one for the hydrogen loss channel of ionized methylhydrazine. This isomer is approximatively 30 kJ mol^{-1} lower in energy than $CH_3NNH_2^+$ and CH_3NHNH^+ at the mG3 level of theory. The $T_{0.5}$ value associated with H loss is 81 meV (van Garderen et al.[4] reported a similar KER, $T_{0.5}$ = 75 meV), indicating that this reaction is unlikely to proceed with a large reverse energy barrier. In the CID mass spectrum of the methylhydrazine ion, fragment ions *m*/*z* 31 and *m*/*z* 30 are observed corresponding to $N_2H_3^+$ and $N_2H_2^{+\bullet}$, respectively. These two ions are also observed in the first crossover region of the breakdown curve of methylhydrazine ions. Fragment ion *m*/*z* 31 corresponds to the loss of a methyl radical to form $NHNH_2^+$ ($T_{0.5}$ = 63 meV) while fragment ion *m*/*z* 30 corresponds to a rearrangement leading to the loss of methane. Three isomeric structures are possible for *m*/*z* 30: iso-diazene ($NNH_2^{+\bullet}$), trans-diazene, or cis-diazene ($HNNH^{+\bullet}$). The structure of this fragment ion has been determined from the VTST fits of the methylhydrazine ion breakdown curves (see Variational Fits) to be either iso-diazene or trans-diazene.

The tetramethylhydrazine ion has only one peak in its MIKE mass spectrum at *m*/*z* 73 corresponding to the loss of a methyl radical to form $(CH_3)_2NNCH_3^+$. The $T_{0.5}$ value associated with the reaction is only 13 meV, indicating that this reaction does not proceed with a reverse energy barrier. In the breakdown diagram of the tetramethylhydrazine ion, another fragment ion is observed in the first crossover region corresponding to fragment ion *m*/*z* 72, which is due to methane loss. Nine possible isomers (five linear and four cyclic)[12,25] of fragment ion *m*/*z* 72 have been considered and are shown in Figure 2.

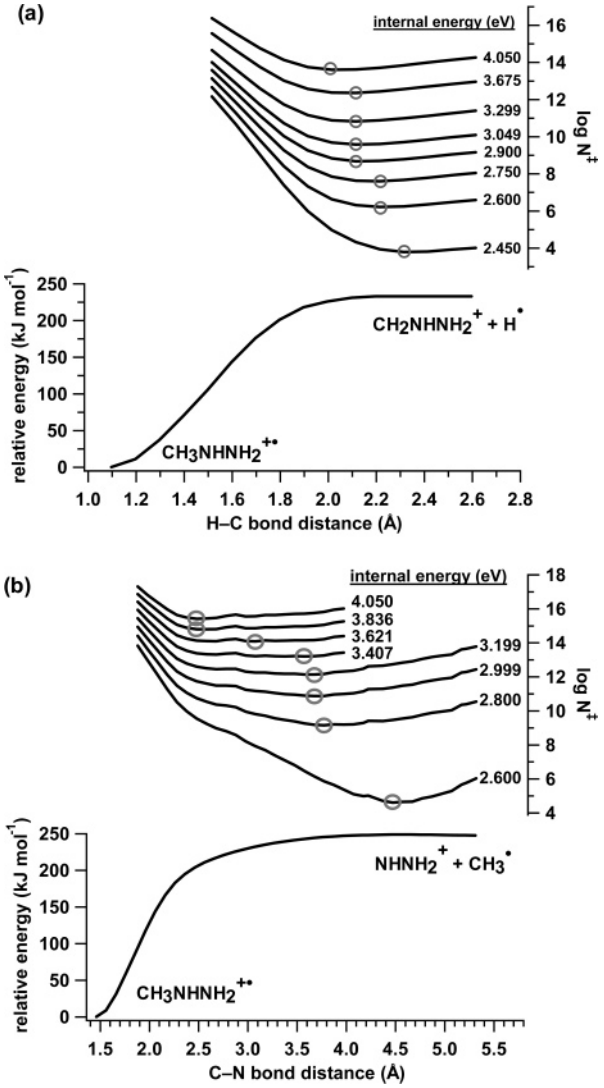

Figure 3. Potential energy curves, calculated at the B3-LYP/6-31+G(d) level of theory, for (a) the loss of a hydrogen atom from the methylhydrazine ion and the sum-of-states as a function of the C−H bond distance and (b) the loss of a methyl radical from the methylhydrazine ion and the sum-of-states as a function of the C−N bond distance. The transition states are identified by circles and correspond to minima in the sum-of-states ($N^{\ddagger}_{min}$).

Locating the Transition States. The relative energies of methylhydrazine and tetramethylhydrazine ions and their fragment ions and neutrals have been calculated at the B3-LYP/6-31+G(d) level of theory and with modified G3 protocol (Table 1).

The potential energy curves for the two unimolecular dissociations of the methylhydrazine ion have been calculated at the B3-LYP/6-31+G(d) level of theory. Figure 3a,b shows the potential energy curves along with the sum-of-states graphs as a function of the C−X bond distance (X = H or N). The transition states for each dissociation channel were identified by finding the minimum in the sum-of-states as a function of internal energy (Tables 2 and 3 and Supporting Information S1 and S2).

The tetramethylhydrazine ion has two low-energy dissociation channels, the loss of a methyl group to form the trimethylhydrazyl fragment ion *m*/*z* 73, $(CH_3)_2NNCH_3^+$, and the rearrangement process leading to the loss of methane and the formation of fragment ion *m*/*z* 72. A potential energy curve and the sum-of-states in the internal energy range of 1.60−4.00 eV for the

TABLE 2: Transition States, Entropies of Activation (600 K), and Energies of Activation (0 K) for the Unimolecular Dissociations of the Methylhydrazine Ion in the Internal Energy Range of 1.90−4.00 eV

dissociation channel				$CH_2NHNH_2^+ + H^\bullet$				
B3-LYP/6-31+G(d)				$\Delta E^a = 2.418$ eV or 233.3 kJ mol^{-1}				
R^* (Å)			1.997	2.097	2.197	2.297		
$\Delta S^{\ddagger b}$ (J K^{-1} mol^{-1})	$I_{CH3} = 3.0$ amu Å^2		−13.56	−10.39	−7.13	−4.01		
	$I_{CH3} = 3.1$ amu Å^2		−13.70	−10.52	−7.26	−4.14		
E_0 (eV)			2.347	2.392	2.412	2.419		
corrected to mG3 product energy				$\Delta E = 2.240$ eV or 216.2 kJ mol^{-1}				
R^* (Å)			1.997	2.097	2.197	2.297		
$\Delta S^{\ddagger}$ (J K^{-1} mol^{-1})	$I_{CH3} = 3.0$ amu Å^2		−13.56	−10.39	−7.13	−4.01		
	$I_{CH3} = 3.1$ amu Å^2		−13.70	−10.52	−7.26	−4.14		
E_0 (eV)			2.169	2.214	2.234	2.241		
fit 1				$\Delta E = 2.193$ eV or 211.6 kJ mol^{-1}				
R^* (Å)			1.997	2.097	2.197	2.297	2.397	
$\Delta S^{\ddagger}$ (J K^{-1} mol^{-1})	$I_{CH3} = 3.0$ amu Å^2		19.72	23.06	26.46	29.69	32.71	
	$I_{CH3} = 3.1$ amu Å^2		19.58	22.93	26.32	29.55	32.58	
E_0 (eV)			2.122	2.167	2.187	2.194	2.195	
fit 2				$\Delta E = 2.201$ eV or 212.4 kJ mol^{-1}				
R^* (Å)			1.997	2.097	2.197	2.297		
$\Delta S^{\ddagger}$ (J K^{-1} mol^{-1})	$I_{CH3} = 3.0$ amu Å^2		22.69	26.02	29.42	32.65		
	$I_{CH3} = 3.1$ amu Å^2		22.56	25.88	29.28	32.52		
E_0 (eV)			2.130	2.175	2.195	2.202		
fit 3				$\Delta E = 2.213$ eV or 213.5 kJ mol^{-1}				
R^* (Å)			1.997	2.097	2.197	2.297		
$\Delta S^{\ddagger}$ (J K^{-1} mol^{-1})	$I_{CH3} = 3.0$ amu Å^2		25.80	29.21	32.61	35.85		
	$I_{CH3} = 3.1$ amu Å^2		25.66	29.08	32.48	35.72		
E_0 (eV)			2.142	2.187	2.207	2.214		

dissociation channel	$NHNH_2^+ + CH_3^\bullet$									
B3-LYP/6-31+G(d)				$\Delta E^a = 2.578$ eV or 248.7 kJ mol^{-1}						
R^* (Å)	2.461	2.561	2.661	3.061	3.561	3.661	3.761	4.061	4.361	4.461
$\Delta S^{\ddagger}$ (J K^{-1} mol^{-1})	13.32	16.29	19.31	30.65	42.70	44.86	46.98	53.46	60.20	62.21
E_0 (eV)	2.112	2.184	2.241	2.401	2.514	2.529	2.541	2.566	2.576	2.578
corrected to mG3 product energy				$\Delta E = 2.725$ eV or 262.9 kJ mol^{-1}						
R^* (Å)	2.561	2.661	3.061	3.561	3.661	3.761	4.061	4.561		
$\Delta S^{\ddagger}$ (J K^{-1} mol^{-1})	16.29	19.31	30.65	42.70	44.86	46.98	53.46	64.21		
E_0 (eV)	2.330	2.388	2.548	2.661	2.675	2.687	2.712	2.725		
fit 1[c]				$\Delta E = 2.528$ eV or 243.9 kJ mol^{-1}						
R^* (Å)	2.561	3.061	3.761	4.061	4.461					
$\Delta S^{\ddagger}$ (J K^{-1} mol^{-1})	17.24	31.64	52.34	58.83	67.62					
E_0 (eV)	2.134	2.351	2.491	2.516	2.528					
fit 2				$\Delta E = 2.528$ eV or 243.9 kJ mol^{-1}						
R^* (Å)	2.561	3.061	3.761	4.061	4.461					
$\Delta S^{\ddagger}$ (J K^{-1} mol^{-1})	19.25	33.71	53.52	60.01	68.81					
E_0 (eV)	2.134	2.351	2.491	2.516	2.528					
fit 3				$\Delta E = 2.528$ eV or 243.9 kJ mol^{-1}						
R^* (Å)	2.561	3.061	3.761	4.061	4.461					
$\Delta S^{\ddagger}$ (J K^{-1} mol^{-1})	20.68	35.18	55.17	61.67	70.47					
E_0 (eV)	2.134	2.351	2.491	2.516	2.528					

dissociation channel	$N_2H_2^{+\bullet} + CH_4$[d]
fit 1[c]	
$\Delta S^{\ddagger}$ (J K^{-1} mol^{-1})	17.26
E_0 (eV)	2.350
fit 2	
$\Delta S^{\ddagger}$ (J K^{-1} mol^{-1})	20.48
E_0 (eV)	2.350
fit 3	
$\Delta S^{\ddagger}$ (J K^{-1} mol^{-1})	20.48
E_0 (eV)	2.350

[a] Energy difference between the equilibrium ion and the plateau on the potential energy curve (energy value taken at $R_{C-H} = 2.597$ Å and $R_{C-N} = 4.561$ Å). [b] $\Delta S^{\ddagger}$ calculated using the free rotor model from East and Radom procedure[24] on the calculations of the third-law entropies. Two values for the moment of inertia of the methyl group have been used giving slightly different results. [c] Fit 1 for methyl and methane losses corresponds to fit 1 for hydrogen loss, etc. [d] Rearrangement process, transition state estimated, see text for explanations.

methyl loss channel have been calculated at the B3-LYP/6-31+G(d) level of theory from the equilibrium geometry up to a C−N bond distance of 3.266 Å. These two graphs are shown in Figure 4.

Fitting the Breakdown Diagrams. The methylhydrazine and tetramethylhydrazine ion breakdown curves were recorded between $h\nu = 9.60-31.95$ eV and $h\nu = 7.74-29.94$ eV, respectively. Eighteen and twenty-five fragment ions have been observed in the methylhydrazine and tetramethylhydrazine ions breakdown curves, respectively. The value of the adiabatic ionization energy (IE_a) employed to calculate the internal energy range of each breakdown curve was found to have a significant impact on the fit of the breakdown curves and on the values of the enthalpy of formation of the product ions. Meot-Ner et al.[26]

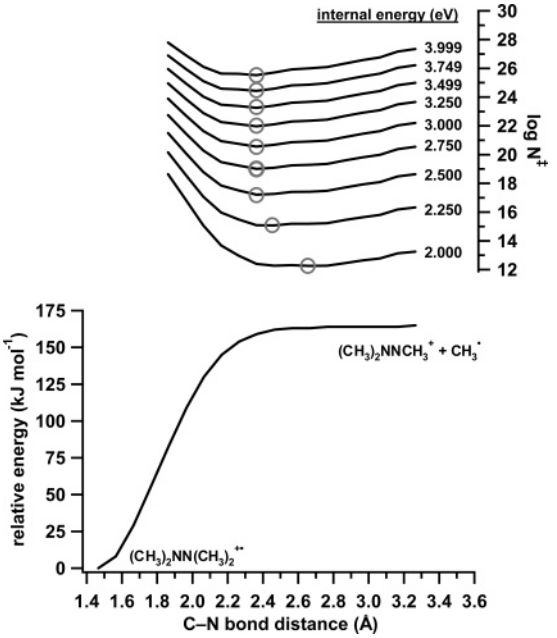

Figure 4. Potential energy curve, calculated at the B3-LYP/6-31+G-(d) level of theory, for the loss of a methyl radical from the tetramethylhydrazine ion and the sum-of-states as a function of the C−N bond distance. The transition states are identified by circles and correspond to minima in the sum-of-states ($N^{\ddagger}_{min}$).

have reported experimental IE_a for methylhydrazine and tetramethylhydrazine ions: 7.70 ± 0.15 eV for MH and 6.78 ± 0.04 eV for TMH. Their methylhydrazine IE_a agrees well with our mG3 calculated IE_a of 7.64 eV.[14] However, their value for tetramethylhydrazine is ∼0.25 eV lower than our calculated mG3 IE_a of 7.02 eV.[11] Depending on the IE_a value used, the internal energy range is shifted by ∼0.25 eV. We found during our fitting process of the breakdown curves of the TMH ion that the calculated mG3 IE_a produced product ion enthalpies of formation more in line with theory than the experimental IE_a determined by Meot-Ner et al.[26] (see Table 6). We cannot explain the discrepancy between our calculated mG3 IE_a and the experimental IE_a reported by Meot-Ner et al.[26] The calculated (mG3) IE_a[11,14] for methylhydrazine and 1,1-dimethylhydrazine agree with their reported values and gave product ion enthalpies of formation consistent with theory.

To fit the methylhydrazine and tetramethylhydrazine ion breakdown curves, we have used the same VTST procedure as described in our previous study of the fragmentation of 1,1-dimethylhydrazine ions.[15] The results for all these fits are summarized in Tables 2 and 3 and the resulting fits are shown in Figures 5 and 6. Only small changes were needed to the energy of the potential energy curves relative to the mG3 results to obtain satisfactory fits.

In all four breakdown curves of ionized methylhydrazine, the hydrogen loss channel has been fitted in the internal energy range of 1.90−2.80 eV. Data for the methyl and methane losses channels were only collected for a parent ion residence time of 1.116 μs and were fitted up to 3.50 eV. At the B3-LYP/6-31+G-(d) level of theory, ten transition states were found in the internal energy range of 1.90−4.00 eV for the methyl loss channel. This was reduced to a more practical five to carry out the fitting (Table 2), and the quality of the fits has not been affected by that simplification.

The $\Delta S^{\ddagger}(45)_{MH}$ values for the hydrogen loss channel ranged from 46 J K^{-1} mol^{-1} at $E_{int} \approx 2.25$ eV to 23 J K^{-1} mol^{-1}at $E_{int} \approx 4.00$ eV. These values are larger than those derived for the hydrogen loss channel in our previous study of the 1,1-dimethylhydrazine ions[15] at the same level of theory ($\Delta S^{\ddagger}(59)_{UDMH}$ = 26 J K^{-1} mol^{-1} at E_{int} = 2.32 eV to 16 J K^{-1} mol^{-1} at E_{int} = 3.56 eV). For methyl loss, the $\Delta S^{\ddagger}(31)_{MH}$ ranges from 70 J K^{-1} mol^{-1} at $E_{int} \approx 2.58$ eV to 17 J K^{-1} mol^{-1} at $E_{int} \approx 4.00$ eV. These values are similar to those derived for the methyl loss channel of 1,1-dimethylhydrazine ions[15] with the only difference being the internal energy range ($\Delta S^{\ddagger}(45)_{UDMH}$ = 65 J K^{-1} mol^{-1} at E_{int} = 2.32 eV to 29 J K^{-1} mol^{-1} at E_{int} = 3.56 eV). The $\Delta S^{\ddagger}$ for the methane loss channel of MH ion ranges from 17.3−20.5 J K^{-1} mol^{-1} (depending on the fit used). $\Delta S^{\ddagger}(30)_{MH}$ does not vary with the internal energy because only one estimated transition state was used to fit the experimental curve of *m*/*z* 30.

For the tetramethylhydrazine ion, at $E_{int} \approx 1.80$ eV, $\Delta S^{\ddagger}(73)_{TMH}$ for the loss of a methyl radical is 39 J K^{-1} mol^{-1} and decreases to 23 J K^{-1} mol^{-1} at E_{int} = 4.00 eV. For the methane loss channel (fragment ion *m*/*z* 72), the entropy of activation decreases from ∼12.7 J K^{-1} mol^{-1} between E_{int} = 1.80 to ∼3.30 eV to approximately −22.9 J K^{-1} mol^{-1} between $E_{int} \approx 3.30$ to 4.00 eV. Because the methane loss reaction necessarily involves a rearrangement, it is curious that two very distinct transition states were needed to obtain a satisfactory fit to the experimental data for this channel. Methane loss is a fairly minor process and so it is possible that the need for two transition states is simply an artifact of the fitting procedure. If it is not, though, it could indicate that the reaction proceeds via two distinct mechanisms depending on the internal energy.

If we compare the $\Delta S^{\ddagger}$ for methyl loss from the three ions we see that as methyl substitution increases on the hydrazine backbone, the $\Delta S^{\ddagger}$ values decrease: $\Delta(\Delta S^{\ddagger}(31)_{MH})$ = 53 J K^{-1} mol^{-1} with ΔE_{int} = 1.42 eV, $\Delta(\Delta S^{\ddagger}(45)_{UDMH})$ = 36 J K^{-1} mol^{-1} with ΔE_{int} = 1.24 eV and $\Delta(\Delta S^{\ddagger}(73)_{TMH})$ = 16 J K^{-1} mol^{-1} with ΔE_{int} = 2.20 eV. This is likely due to the remaining, post-dissociation, steric hindrance of the methyl torsions as methyl-substitution increases.

Appearance Energies. Eighteen and twenty-five fragment ions have been observed in the breakdown curves of ionized methylhydrazine and tetramethylhydrazine, respectively, from threshold up to h$\nu \approx$ 32 eV. Tentative structures or empirical formulas have been assigned to each fragment ion and can be found in Tables 4 and 5. These tables also contain the previous experimental appearance energies as well as an indication of the ionization technique used to generate the fragment ions. Figures 7 and 8 show the relative abundances of all fragment ions of MH and TMH ions as a function of photon energy. In the breakdown curve of methylhydrazine, a fragment ion was observed at *m*/*z* 32. Because this ion was not observed in the MIKE and CID mass spectra of $CH_3NHNH_2^{+\bullet}$, it was assumed to be due to an impurity and its AE has not been reported in Table 4. In the breakdown diagram of tetramethylhydrazine ion, we observed fragment ions at *m*/*z* 86 and *m*/*z* 87 corresponding to H losses, but it was not feasible to determine reliable AEs for these ions from the TPEPICO data. An ion at *m*/*z* 74 was also observed but was attributed to a decomposition byproduct.

Figure 9 shows portions of the time-of-flight (TOF) spectra of methylhydrazine recorded at photon energies of 24.45 and 30.95 eV. In the spectrum recorded at 24.45 eV, the peaks are well resolved and can be associated with fragments possessing relatively small kinetic energies. An AE of 27.95 eV has been determined for the doubly charged parent ion in the present work. The observation of the doubly charged ion (*m*/*z* 22.5) indicates that at least some of these species have lifetimes greater than the few microseconds required to reach the detector. In

TABLE 3: Transition States, Entropies of Activation (600 K), and Energies of Activation (0 K) for the Unimolecular Dissociations of the Tetramethylhydrazine Ion in the Internal Energy Range of 1.60−4.00 eV[a]

dissociation channel	$(CH_3)_2NNCH_3^+ + CH_3^\bullet$		
B3-LYP/6-31+G(d)	$\Delta E^b = 1.706$ eV or 165 kJ mol^{-1}		
R^* (Å)	2.366	2.466	2.666	2.766
$\Delta S^\ddagger$ (J K^{-1} mol^{-1})	5.12	8.48	14.14	17.52
E_0 (eV)	1.650	1.675	1.694	1.698
corrected to mG3 product energy	$\Delta E = 1.757$ eV or 170 kJ mol^{-1}		
R^* (Å)	2.366	2.466	2.766
$\Delta S^\ddagger$ (J K^{-1} mol^{-1})	5.12	8.48	17.52
E_0 (eV)	1.701	1.726	1.749
fit 1[c]	$\Delta E = 1.816$ eV or 175 kJ mol^{-1}		
R^* (Å)	2.366	2.466	2.766
$\Delta S^\ddagger$ (J K^{-1} mol^{-1})	25.10	28.47	37.51
E_0 (eV)	1.760	1.785	1.808
fit 2	$\Delta E = 1.806$ eV or 174 kJ mol^{-1}		
R^* (Å)	2.366	2.466	2.766
$\Delta S^\ddagger$ (J K^{-1} mol^{-1})	24.03	27.39	36.44
E_0 (eV)	1.750	1.775	1.798
fit 3	$\Delta E = 1.831$ eV or 177 kJ mol^{-1}		
R^* (Å)	2.366	2.466	2.766
$\Delta S^\ddagger$ (J K^{-1} mol^{-1})	26.25	29.61	38.66
E_0 (eV)	1.775	1.800	1.823
fit 4	$\Delta E = 1.791$ eV or 173 kJ mol^{-1}		
R^* (Å)	2.366	2.466	2.766
$\Delta S^\ddagger$ (J K^{-1} mol^{-1})	23.02	26.39	35.43
E_0 (eV)	1.735	1.760	1.783

dissociation channel	$C_3H_8N_2^{+\bullet} + CH_4$	
fit 1[c]		
estimated TS[d]	1	2
$\Delta S^\ddagger$ (J K^{-1} mol^{-1})	14.16	−18.76
E_0 (eV)	2.000	1.500
fit 2		
estimated TS	1	2
$\Delta S^\ddagger$ (J K^{-1} mol^{-1})	11.78	−24.62
E_0 (eV)	2.000	1.400
fit 3		
estimated TS	1	2
$\Delta S^\ddagger$ (J K^{-1} mol^{-1})	12.94	−23.28
E_0 (eV)	2.000	1.400
fit 4		
estimated TS	1	2
$\Delta S^\ddagger$ (J K^{-1} mol^{-1})	11.78	−25.39
E_0 (eV)	2.000	1.400

[a] Internal energy range when $IE_a = 7.02$ eV.[11] [b] Energy difference between the equilibrium ion and the plateau on the potential energy surface (energy value taken at $R_{C-N} = 3.266$ Å). [c] Fit 1 for methyl loss corresponds to fit 1 for methane loss, etc. [d] Estimated TS 1 ranging from $E_{int} = 1.60$ eV to ~3.20−3.40 eV and estimated TS 2 from $E_{int} \approx 3.20-3.40$ to 4.00 eV.

the spectrum recorded at 30.95 eV, which is above the threshold for double ionization, some of the peaks have broadened substantially and must be attributed to fragments possessing significant kinetic energies. This broadening is particularly evident in the peaks corresponding to the CH_3^+ and $NHNH_2^+$ fragments. The large kinetic energy probably results from a charge separation reaction in the doubly charged parent ion yielding two singly charged species. The large kinetic energy is due to a Coulomb explosion between the initial ion-pair. A triplet profile is observed in the TOF peak shape for the CH_3^+ fragment in the spectrum recorded at 30.95 eV. The central peak corresponds to fragment ions formed directly with very little kinetic energy. The other two peaks correspond to CH_3^+ fragments formed with large kinetic energies, (probably a few eV, via a Coulomb explosion) and directed predominantly toward or away from the channelplate detector. Energetic fragments ejected in directions approximately perpendicular to the spectrometer axis are lost on apertures along the flight path, thereby producing dips in the TOF peak profile.

Thermochemistry. The $\Delta_f H_0$ for the fragment ions (*m*/*z* 73, *m*/*z* 72, *m*/*z* 45, *m*/*z* 31, and *m*/*z* 30) have been determined from the variational fits of the breakdown curves and from the mG3 calculations. These results are listed in Table 6 along with reported values. The enthalpies of formation have been determined from the following equations:[19]

$$AB + e^- \rightarrow AB^{+\bullet} + 2e^- \quad (3)$$

$$AB^{+\bullet} \rightarrow A^+ + B^\bullet \quad (4)$$

$$\Delta_f H_0(A^+) = E_0(A{-}B^{+\bullet}) + \Delta_f H_0(AB^{+\bullet}) - \Delta_f H_0(B^\bullet) \quad (5)$$

The $\Delta_f H_0$ of the parent ion $AB^{+\bullet}$ and neutral fragment $B^\bullet$ were taken from our mG3 calculations (Table 6). To calculate $\Delta_f H_0$ from the VTST results, we have used the procedure described in our prior study of 1,1-dimethylhydrazine ions.[15] The E_0 for the transition state found at the lowest internal energy studied was used. Uncertainties in the enthalpy of formation arise from the uncertainties in IE_a, the E_0, and the photon energy.

The adiabatic ionization energy has a direct effect on the value of the enthalpy of formation as discussed previously. Using the Meot-Ner et al.[26] IE_a for tetramethylhydrazine gave a $\Delta_f H_0$ of

TABLE 4: Appearance Energies for Fragment Ions from Methylhydrazine

m/z	fragment ion	AE (eV)	ionization technique	ref
45	$CH_2NHNH_2^+$	9.85 ± 0.05	TPEPICO	present work
	$CH_5N_2^+$	10.2 ± 0.1	electron ionization	Dibeler et al.[8]
		10.18 ± 0.1	electron ionization	Foner and Hudson[30]
		9.2 ± 0.1	photoionization	Akopyan and Vilesov[31]
	$CH_3NNH_2^+$	10	electron ionization	Syage[32]
44	$CH_4N_2^+$	12.45 ± 0.10	TPEPICO	present work.
		10.4 ± 0.2	electron ionization	Dibeler et al.[8]
		10.5	electron ionization	Syage[32]
		9.92 ± 0.1	electron ionization	Foner and Hudson[30]
		9.4 ± 0.1	photoionization	Akopyan and Vilesov[31]
	$CH_3N_2H^+$	10.5	electron ionization	Syage[32]
43	$CH_3N_2^+$	13.85 ± 0.20	TPEPICO	present work
		11.9 ± 0.3	electron ionization	Dibeler et al.[8]
		14.8 ± 0.3	electron ionization	Dibeler et al.[8]
		9.2 ± 0.2	photoionization	Akopyan and Vilesov[31]
		11.5	electron ionization	Syage[32]
42	$CH_2N_2^+$	17.45 ± 0.20	TPEPICO	present work
		15.2 ± 0.2	electron ionization	Dibeler et al.[8]
		16.5	electron ionization	Syage[32]
41	CHN_2^+	22.95 ± 0.50	TPEPICO	present work
		28	electron ionization	Syage[32]
31	$H_3N_2^+$	10.25 ± 0.05	TPEPICO	present work
		10.7 ± 0.3	electron ionization	Dibeler et al.[8]
		11	electron ionization	Syage[32]
		9.82	electron ionization	Burgers et al.[1]
		9.5 ± 0.1	photoionization	Akopyan and Vilesov[31]
	CH_5N^+	11.3 ± 0.1	photoionization	Akopyan and Vilesov[31]
30	$H_2N_2^+$	10.05 ± 0.05	TPEPICO	present work
		11.2 ± 0.2	electron ionization	Dibeler et al.[8]
	$CH_2NH_2^+$	11.5	electron ionization	Syage[32]
29	CH_3N^+ or N_2H^+	11.65 ± 0.10	TPEPICO	present work
	HN_2^+	13.3 ± 0.3	electron ionization	Dibeler et al.[8]
	$CHNH_2^+$	12.5	electron ionization	Syage[32]
28	CH_2N^+ or N_2^+	12.35 ± 0.10	TPEPICO	present work
		13.2 ± 0.3	electron ionization	Dibeler et al.[8]
	$CHNH^+$	12	electron ionization	Syage[32]
27	CHN^+	20.45 ± 0.40	TPEPICO	present work
		24	electron ionization	Syage[32]
22.5	$CH_5N_2^{2+}$	27.95 ± 1.00	TPEPICO	present work
		36	electron ionization	Syage[32]
18	NH_4^+	12.25 ± 0.10	TPEPICO	present work
		10.5	electron ionization	Syage[32]
17	NH_3^+	11.95 ± 0.10	TPEPICO	present work
		12	electron ionization	Syage[32]
16	CH_4^+ or NH_2^+	15.85 ± 0.20	TPEPICO	present work
	NH_2^+	14.5	electron ionization	Syage[32]
15	CH_3^+ or NH^+	14.45 ± 0.20	TPEPICO	present work
		14.1 ± 0.3	electron ionization	Dibeler et al.[8]
		14	electron ionization	Syage[32]
14	CH_2^+ or N^+	19.90 ± 0.25	TPEPICO	present work
	CH_2^+	22	electron ionization	Syage[32]
13	CH^+	22.95 ± 0.50	TPEPICO	present work
		24	electron ionization	Syage[32]
12	C^+	26.95 ± 1.00	TPEPICO	present work
		33	electron ionization	Syage[32]

the product ion, $(CH_3)_2NNCH_3^+$, that did not agree with our calculated mG3 value (Table 6). Using $IE_a = 6.78 \pm 0.04$ eV,[26] the derived $\Delta_f H_0$ of $(CH_3)_2NNCH_3^+$ was 854 ± 7 kJ mol^{-1}, which is 25 kJ mol^{-1} higher than our calculated mG3 value of 829 kJ mol^{-1}. Again, using our calculated mG3 IE_a of 7.02 eV[11] the $\Delta_f H_0$ of the trimethylhydrazyl ion was found to be 833 ± 5 kJ mol^{-1}. Dibeler et al.[8] reported an experimental $\Delta_f H$ of $(CH_3)_2NNCH_3^+$ that is 9−13 kJ mol^{-1} lower than our mG3 or VTST values.

The derived $\Delta_f H_0$ of $CH_2NHNH_2^+$, using the mG3 IE_a = 7.64 eV[11,14] to fit the breakdown curve of ionized methylhydrazine, gave a value of 862 ± 5 kJ mol^{-1}, which is in very good agreement with our calculated mG3 value of 864 kJ mol^{-1}. For the fragment ion *m*/*z* 45 from the methylhydrazine ion, Dibeler et al.[8] reported a $\Delta_f H$ that is 5−10 kJ mol^{-1} lower than our determined values. However, they did not suggest any structure for this ion. Burgers et al.[1] reported a $\Delta_f H_0$ for $CH_2NHNH_2^+$ based on its appearance energy from the 2-hydrazinoethanol ion (AE = 9.1 eV)[1], which is 48 kJ mol^{-1} lower than our calculated mG3 enthalpy of formation. The group[4] later reported a revised $\Delta_f H_0$ for $CH_2NHNH_2^+$, which is only 10 kJ mol^{-1} lower than our mG3 value. Nguyen[3] calculated the $\Delta_f H_{298}$ of $CH_2NHNH_2^+$ to be 860 ± 12 kJ mol^{-1} at the MP4SDTQ/6-311++G(2d,2p) level of theory, which is 14 kJ mol^{-1} higher than our calculated 298 K mG3 value of 846 kJ mol^{-1}.

For the fragment ion *m*/*z* 31 ($NHNH_2^+$), the $\Delta_f H_0$ was calculated from the VTST fits to be 959 ± 5 kJ mol^{-1}, which is 18 kJ mol^{-1} lower our calculated mG3 $\Delta_f H_0$ of 976 kJ mol^{-1}.

TABLE 5: Appearance Energies for Fragment Ions from Tetramethylhydrazine

m/z	fragment ion	AE (eV)	ionization technique	ref
87	$C_4H_{11}N_2^+$		TPEPICO	present work
86	$C_4H_{10}N_2^+$		TPEPICO	present work.
73	$C_3H_9N_2^+$	8.79 ± 0.05	TPEPICO	present work
		9.1 ± 0.1	electron ionization	Dibeler et al.[8]
72	$C_3H_8N_2^+$	9.14 ± 0.05	TPEPICO	present work
		8.9 ± 0.1	electron ionization	Dibeler et al.[8]
71	$C_3H_7N_2^+$	10.04 ± 0.05	TPEPICO	present work
		10.7 ± 0.1	electron ionization	Dibeler et al.[8]
58	$C_2H_6N_2^+$	11.44 ± 0.10	TPEPICO	present work
		10.5 ± 0.1	electron ionization	Dibeler et al.[8]
		13.3 ± 0.5	electron ionization	Dibeler et al.[8]
57	$C_2H_5N_2^+$	10.54 ± 0.10	TPEPICO	present work
		12.4 ± 0.2	electron ionization	Dibeler et al.[8]
47	$CH_7N_2^+$ or $C_2H_9N^+$	11.54 ± 0.10	TPEPICO	present work
		17.94 ± 0.50	TPEPICO	present work
46	$CH_6N_2^+$ or $C_2H_8N^+$	11.54 ± 0.10	TPEPICO	present work
		10.9 ± 0.2	electron ionization	Dibeler et al.[8]
		12.3 ± 0.2	electron ionization	Dibeler et al.[8]
45	$CH_5N_2^+$ or $C_2H_7N^+$	11.34 ± 0.10	TPEPICO	present work
		9.7 ± 0.2	electron ionization	Dibeler et al.[8]
44	$CH_4N_2^+$ or $C_2H_6N^+$	11.04 ± 0.10	TPEPICO	present work
		11.2 ± 0.2	electron ionization	Dibeler et al.[8]
		11.2 ± 0.1	electron ionization	Gowenlock et al.[33]
43	$CH_3N_2^+$, $C_2H_5N^+$ or $s-C_3H_7^+$	11.54 ± 0.10	TPEPICO	present work
		10.9 ± 0.2	electron ionization	Dibeler et al.[8]
		13.2 ± 0.3	electron ionization	Dibeler et al.[8]
42	$CH_2N_2^+$ or $C_2H_4N^+$	11.54 ± 0.10	TPEPICO	present work
		12.2 ± 0.2	electron ionization	Dibeler et al.[8]
41	CHN_2^+ or $C_2H_3N^+$	20.44 ± 0.50	TPEPICO	present work
		~13	electron ionization	Dibeler et al.[8]
40	CN_2^+ or $C_2H_2N^+$	20.94 ± 0.50	TPEPICO	present work
39	C_2HN^+		TPEPICO	present work
32	$H_4N_2^+$	11.64 ± 0.10	TPEPICO	present work
		12.3 ± 0.1	electron ionization	Dibeler et al.[8]
31	$H_3N_2^+$	13.04 ± 0.10	TPEPICO	present work
30	$H_2N_2^+$	11.64 ± 0.10	TPEPICO	present work
		11.9 ± 0.2	electron ionization	Dibeler et al.[8]
29	CH_3N^+ or N_2H^+	14.94 ± 0.20	TPEPICO	present work
28	CH_2N^+ or N_2^+	12.14 ± 0.10	TPEPICO	present work
		13.1 ± 0.2	electron ionization	Dibeler et al.[8]
27	CHN^+	14.54 ± 0.20	TPEPICO	present work
26	CN^+ or $C_2H_2^+$	18.94 ± 0.50	TPEPICO	present work
18	NH_4^+	12.24 ± 0.10	TPEPICO	present work
17	NH_3^+	17.94 ± 0.50	TPEPICO	present work
16	CH_4^+ or NH_2^+	19.94 ± 0.50	TPEPICO	present work
15	CH_3^+ or NH^+	14.14 ± 0.20	TPEPICO	present work
		14 ± 1	electron ionization	Dibeler et al.[8]
14	CH_2^+ or N^+	22.94 ± 0.50	TPEPICO	present work

Dibeler et al.[8] reported a $\Delta_f H$ of 992 kJ mol^{-1} that is 16−33 kJ mol^{-1} higher than our $\Delta_f H_0$ values. van Garderen et al.[4] derived the $\Delta_f H_{298}$ of $N_2H_3^+$ from its AE ($CH_3^\bullet$ loss from $CH_3NHNH_2^{+\bullet}$) to be 954 kJ mol^{-1}. Matus et al.[2] calculated the $\Delta_f H_0$ of $N_2H_3^+$ to be 969 kJ mol^{-1} at the CCSD(T) level of theory, and their results are in excellent agreement with our own calculated $\Delta_f H$. Nguyen[3] reported a $\Delta_f H_{298}$ for $NHNH_2^+$ of 974 ± 8 kJ mol^{-1} at the MP4SDTQ/6-311++G(2d,2p) level of theory, which is 9 kJ mol^{-1} higher than our 298 K mG3 calculated $\Delta_f H$ of 965 kJ mol^{-1}. The fragment ion *m*/*z* 30 ($N_2H_2^{+\bullet}$) has a VTST $\Delta_f H_0$ of 1155 ± 5 kJ mol^{-1}. Given the presence of a barrier to this reaction, it is safe to assume that this value is an upper limit to the true value, and hence we can rule out the cis-$HNNH^+$ ion structure. Thus, ion *m*/*z* 30 could be either the iso-diazene ion ($H_2NN^{+\bullet}$) or the trans-diazene ion ($HNNH^{+\bullet}$). A more thorough computational study of the mechanism would be needed to confirm the ion structure. Dibeler et al.[8] reported a $\Delta_f H$ for this fragment ion (1247 kJ mol^{-1}) that is much higher than our calculated mG3 $\Delta_f H_0$ for all three $N_2H_2^{+\bullet}$ isomers.

The $\Delta_f H_0$ for the fragment ion *m*/*z* 72, $C_3H_8N_2^{+\bullet}$, has been calculated from the VTST fits and mG3 calculations. The VTST derived $\Delta_f H_0$ is 1064 ± 5 kJ mol^{-1}, which is 68−124 kJ mol^{-1} higher than the mG3 calculated $\Delta_f H_0$ of the five linear isomers of $C_3H_8N_2^{+\bullet}$ and 120−203 kJ mol^{-1} higher than the mG3 calculated $\Delta_f H_0$ values of the cyclic isomers VIII and IX (Figure 2). Cyclic isomers VI and VII have a $\Delta_f H_0$ of 1055 and 1051 kJ mol^{-1}, respectively, which are both in reasonable agreement with our VTST derived value. Obviously, there is a large barrier to methane loss in ionized TMH, and the fitting procedure is giving us the height of this barrier and not the true thermochemical threshold to the reaction.

Proton affinities of some NN-containing neutral molecules have been determined from the following equations, using the VTST derived $\Delta_f H_0$ reported above and compared to reported values (Table 7):[27]

$$M + H^+ \rightarrow MH^+ \quad (6)$$

$$PA(M) = -\Delta_{rxn}H = \Delta_f H(M) + \Delta_f H(H^+) - \Delta_f H(MH^+) \quad (7)$$

TABLE 6: Enthalpies of Formation of the Methylhydrazine and Tetramethylhydrazine Ions and of Their Ionic and Neutral Fragments

m/z	ion or neutral	$\Delta_f H$ (kJ mol^{-1})	method	ref
88	$(CH_3)_2NN(CH_3)_2^{+\bullet}$	809	mG3 calculations (0 K)	Boulanger et al.[11]
		772	mG3 calculations (298 K)	Boulanger et al.[11]
73	$(CH_3)_2NNCH_3^+$	833 ± 5	VTST fit (0 K)[a]	present work
		829	mG3 calculations (0 K)	present work
		799	mG3 calculations (298 K)	present work
		820	electron ionization	Dibeler et al.[8]
72	$C_3H_8N_2^{+\bullet}$	1064 ± 5	VTST fit (0 K)[a]	present work
	isomer I	996	mG3 calculations (0 K)	present work
		970	mG3 calculations (298 K)	present work
	isomer II	992	mG3 calculations (0 K)	present work
		966	mG3 calculations (298 K)	present work
	isomer III	966	mG3 calculations (0 K)	present work
		941	mG3 calculations (298 K)	present work
	isomer IV	953	mG3 calculations (0 K)	present work
		928	mG3 calculations (298 K)	present work
	isomer V	940	mG3 calculations (0 K)	present work
		916	mG3 calculations (298 K)	present work
	isomer VI	1055	mG3 calculations (0 K)	present work
		1029	mG3 calculations (298 K)	present work
		≤ 1152	estimated	Holmes et al.[12]
	isomer VII	1051	mG3 calculations (0 K)	present work
		1024	mG3 calculations (298 K)	present work
	isomer VIII	861	mG3 calculations (0 K)	present work
		832	mG3 calculations (298 K)	present work
		≤ 1025	estimated	Holmes et al.[12]
	isomer IX	944	mG3 calculations (0 K)	present work
		916	mG3 calculations (298 K)	present work
46	$CH_3NHNH_2^{+\bullet}$	864	mG3 calculations (0 K)	Boulanger et al.[11,14]
		844	mG3 calculations (298 K)	Boulanger et al.[11,14]
45	$CH_2NHNH_2^+$	862 ± 5	VTST fit (0 K)[b]	present work
		864	mG3 calculations (0 K)	present work
		846	mG3 calculations (298 K)	present work
		816	electron ionization	Burgers et al.[1]
		854	electron ionization	Dibeler et al.[8]
		860 ± 12	ab initio calculations (298 K)	Nguyen.[3]
		854 ± 21	electron ionization	van Garderen et al.[4]
31	$HNNH_2^+$	959 ± 5	VTST fit (0 K)[b]	present work
		976	mG3 calculations (0 K)	present work
		965	mG3 calculations (298 K)	present work
		895	electron ionization	Burgers et al.[1]
		992	electron ionization	Dibeler et al.[8]
		969.0	calculations (0 K)	Matus et al.[2]
		957.7	calculations (298 K)	Matus et al.[2]
		974 ± 8	ab initio calculations (298 K)	Nguyen.[3]
		954	experimental	van Garderen et al.[4]
30	$N_2H_2^{+\bullet}$	1155 ± 5	VTST fit (0 K)[b]	present work
	trans-$HNNH^{+\bullet}$	1147	mG3 calculations (0 K)	present work
		1140	mG3 calculations (298 K)	present work
	iso-$NNH_2^{+\bullet}$	1156	mG3 calculations (0 K)	present work
		1149	mG3 calculations (298 K)	present work
	cis-$HNNH^{+\bullet}$	1171	mG3 calculations (0 K)	present work
		1164	mG3 calculations (298 K)	present work
		1247	electron ionization	Dibeler et al.[8]
	CH_4	−62	mG3 calculations (0 K)	present work
		−70	mG3 calculations (298 K)	present work
	$CH_3^\bullet$	149	mG3 calculations (0 K)	Boulanger et al.[15]
		146	mG3 calculations (298 K)	Boulanger et al.[15]
	$H^\bullet$	216	mG3 calculations (0 K)	Boulanger et al.[15]
		218	mG3 calculations (298 K)	Boulanger et al.[15]

[a] IE_a(TMH) = 7.02 eV, calculated mG3 value from Boulanger et al.[11] [b] IE_a(MH) = 7.64 eV, calculated mG3 value from Boulanger et al.[11,14]

For $N_2H_3^+$, $CH_2NHNH_2^+$, and $CH_3NNH_2^+$,[15] $\Delta_f H_0$ have been derived from the VTST fits of the breakdown curves. Using these enthalpies of formation, a PA was obtained for each reported $\Delta_f H_0$ of the corresponding neutral molecule. The lowest reported PA[4] of trans-N_2H_2 is 764 ± 8 kJ mol^{-1}, which is in good agreement with our determined values (PA ≈ 778 ± 5 kJ mol^{-1} using our VTST $\Delta_f H_0(NHNH_2^+)$ and PA = 768 kJ mol^{-1} using the mG3 $\Delta_f H_0$). The present $\Delta_f H_0$ of $NHNH_2^+$ results in average PA values for NNH_2 (i.e., the bare N atom) and cis-HNNH of 890 ± 5 and ∼ 798 ± 5 kJ mol^{-1}, respectively. There have been no previously reported PAs for these two compounds. Methyldiazene ($CH_3N{=}NH$) has two sites to accept a proton (its substituted nitrogen atom and its terminal nitrogen atom) and thus two different proton affinities. Hunter and Lias[28] reported the PA of each nitrogen to be 845 and 841 kJ mol^{-1}, respectively. These values are in good agreement with the PA

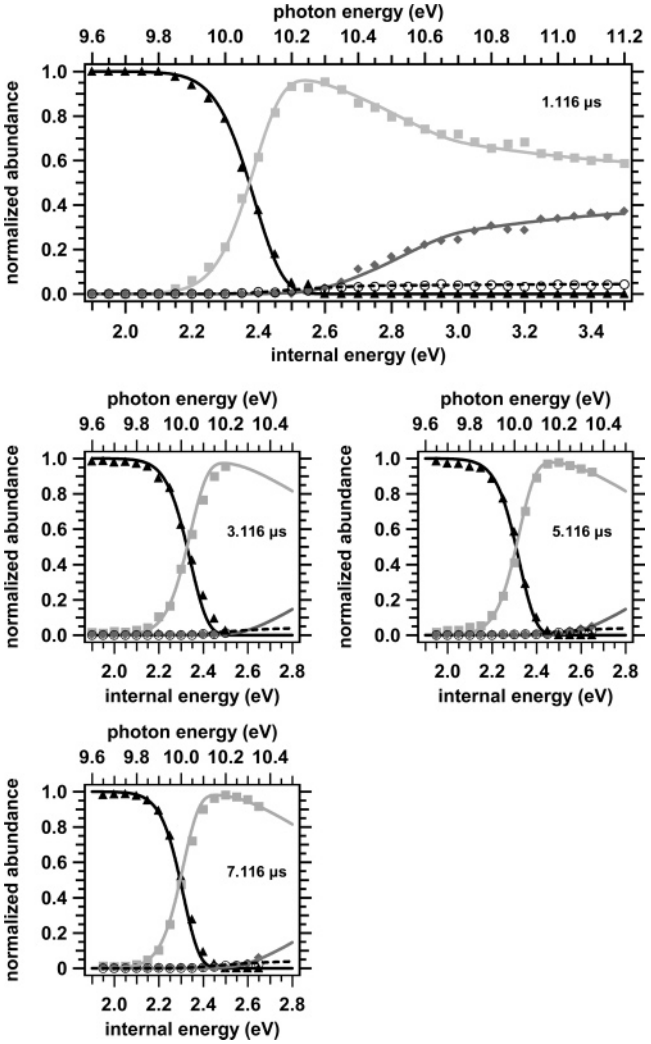

Figure 5. Comparison between the experimental breakdown curve and the theoretical fit (fit 2) using the variational transition states of the hydrogen and methyl losses of the methylhydrazine ion. The parent ion *m*/*z* 46 is represented by a black triangle, the fragment ion *m*/*z* 45 by a light gray square, the fragment ion *m*/*z* 31 by a dark gray diamond, and the fragment ion *m*/*z* 30 is represented by an open circle. The theoretical fits are represented by the solid lines (black for parent ion *m*/*z* 46, light gray for fragment ion *m*/*z* 45 and dark gray for fragment ion *m*/*z* 31) and by a black dashed line for the fragment ion *m*/*z* 30.

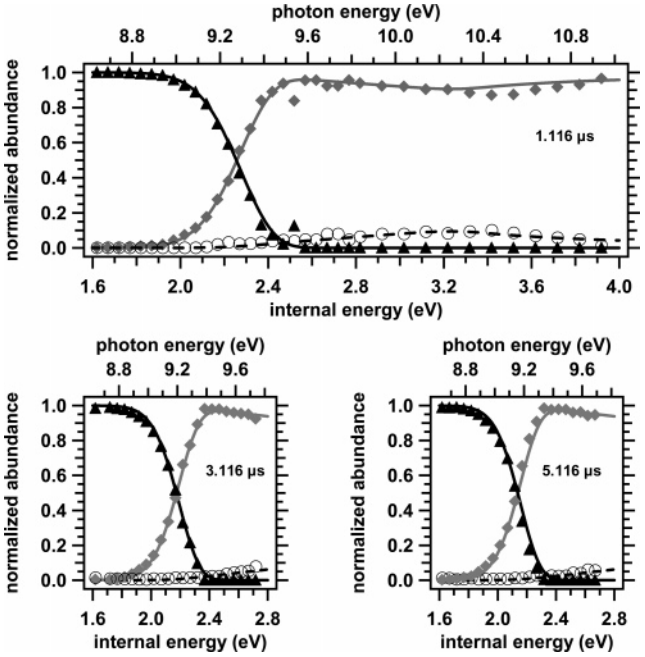

Figure 6. Comparison between the experimental breakdown curves and the theoretical fit (fit 2) using the variational transition states of the methyl loss of the tetramethylhydrazine ion. The parent ion *m*/*z* 88 is represented by a black triangle, the fragment ion *m*/*z* 73 by a dark gray diamond, and the fragment ion *m*/*z* 72 by an open circle. The theoretical fits are represented by the solid lines (black for parent ion *m*/*z* 88 and dark gray for ion *m*/*z* 73) and a black dashed line for fragment ion *m*/*z* 72.

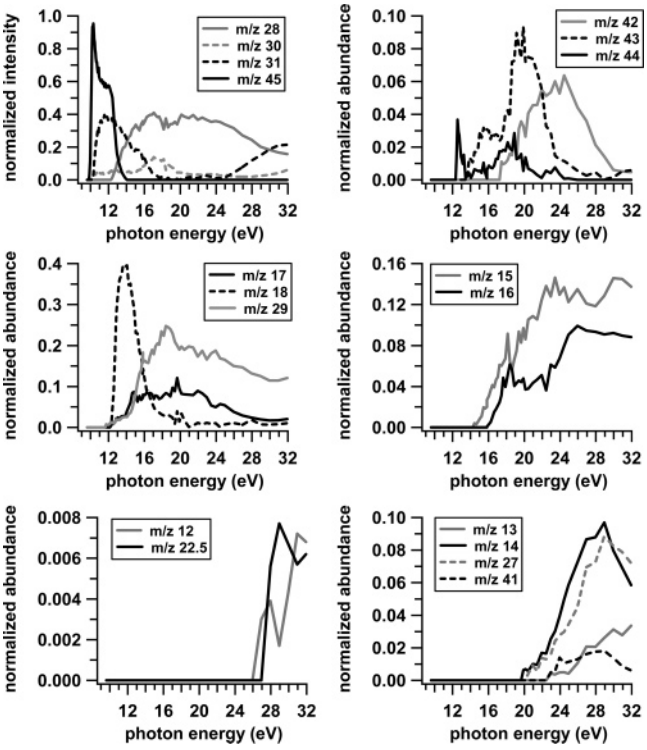

Figure 7. Relative abundances of all fragment ions of methylhydrazine in the photon energy range 9−32 eV.

reported by van Garderen et al.[4] at the SDCI + Pople/6-31G**//6-31G* level of theory: 841 kJ mol^{-1} for the substituted N atom and 845 kJ mol^{-1} for the terminal N atom. However, Nguyen[3] reported a PA for CH_3NNH at the MP4SDTQ/6-311++G(2d,2p) level of theory that is ∼30 kJ mol^{-1} lower than those reported by Hunter and Lias[28] and van Garderen et al.[4] Nguyen's value[3] is in agreement with our calculated mG3 PA of 818 kJ mol^{-1} for the terminal N atom of CH_3NNH, which is slightly higher than that of the substituted one (PA(CH_3**N**NH) = 815 kJ mol^{-1}). The PA of CH_2=NNH_2 has also been calculated to be ∼857 kJ mol^{-1} at the substituted nitrogen atom. The PA at the terminal nitrogen atom is lower, ∼838 kJ mol^{-1}. The carbon proton affinity in CH_2=NNH_2 was calculated to be 809 kJ mol^{-1} using the calculated mG3 enthalpies of formation. The calculated PAs of hydrazine, methylhydrazine, 1,1-dimethylhydrazine, and tetramethylhydrazine using the mG3 procedure are also reported in Table 7. Consistent with trends observed for homologous alkylamines, aliphatic alcohols and bromides,[27] the PA of the substituted nitrogen atom in the hydrazine derivatives increases with increasing methyl substitution. This can be traced to the lowering of the energy of the nitrogen lone pair orbital upon methyl substitution.

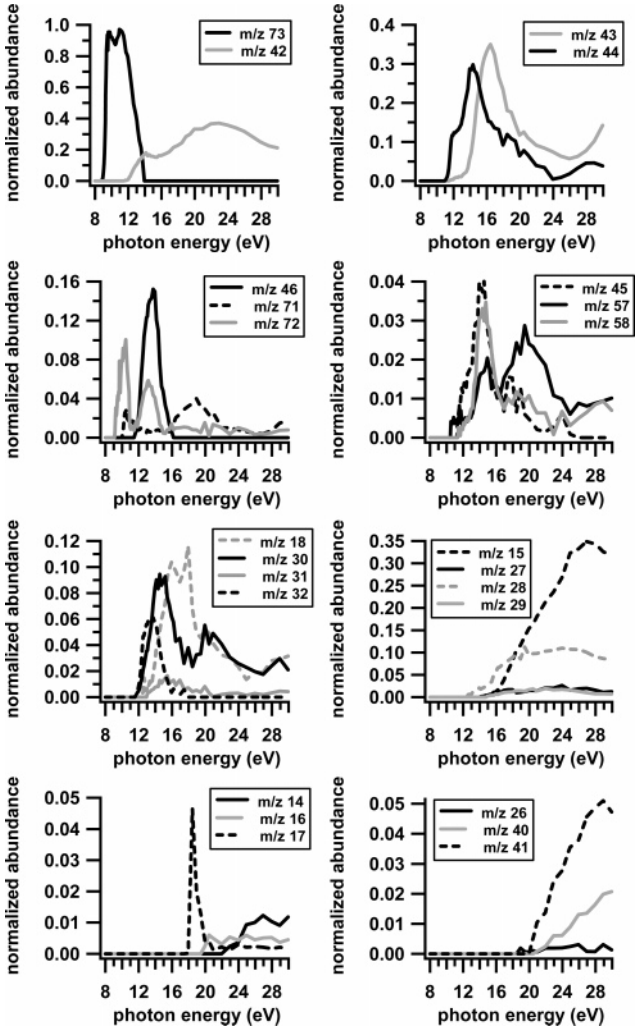

Figure 8. Relative abundances of all fragment ions of tetramethylhydrazine in the photon energy range 8−30 eV.

Bond strengths are important thermochemical values to know to understand the chemical properties of molecules. The bond dissociation enthalpy (DH) of a molecule AB is defined as the enthalpy of the homolytic bond cleavage reaction of the molecule AB and is calculated according to the equations written below:[29]

$$AB \rightarrow A + B \quad (8)$$

$$\Delta_{rxn}H = \Delta_f H(A) + \Delta_f H(B) - \Delta_f H(AB) = DH(A-B) \quad (9)$$

The three methyl-substituted hydrazine ions dissociated by either losing a methyl radical, a hydrogen atom, or both. The N−C or H−C bond dissociation enthalpies in the neutral and ionic hydrazines were derived from the VTST $\Delta_f H_0$ of the product ions and from the calculated mG3 $\Delta_f H_0$ and are listed in Table 8. The N−C bond dissociation enthalpies in the neutral hydrazine derivatives are constant as the methyl substitution increases on the hydrazine backbone showing that the effect of methyl substitution on the stability of the radicals formed from the homolytic bond cleavage reaction is similar to that for the neutral molecules. However, in the radical cations the N−C bond dissociation enthalpy decreases with methyl substitution. The mG3 calculated DH(N−CH_3) decreases from 262 kJ mol^{-1} in the $MH^{+\bullet}$ to 230 kJ mol^{-1} in $UDMH^{+\bullet}$ and to 170 kJ mol^{-1} in $TMH^{+\bullet}$. When the nitrogen−carbon bond is cleaved in the parent radical cation, a singlet fragment ion is formed:

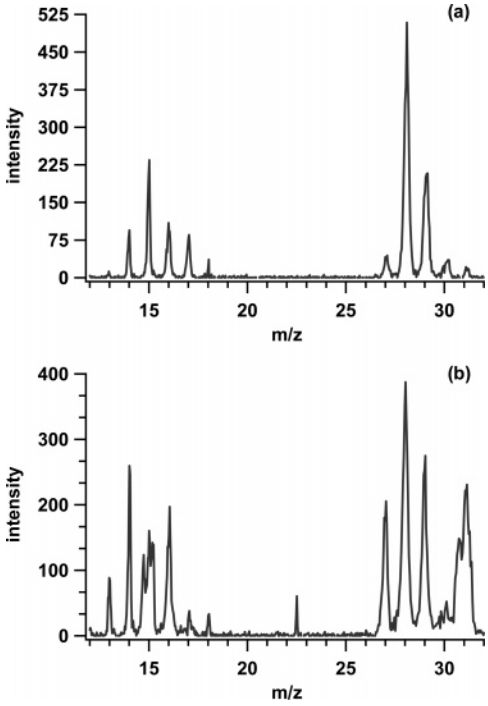

Figure 9. Portions of the TOF mass spectra of methylhydrazine recorded at photon energies of (a) 24.45 eV and (b) 30.95 eV.

$$(CH_3)_2NN(CH_3)_2^{+\bullet} \rightarrow (CH_3)_2NNCH_3^{+} + CH_3^{\bullet} \quad (10)$$

So we can conclude that the positive charge is better stabilized in the fragment ion than in the parent radical cation as the methyl substitution increases on the hydrazine backbone. The H−C bond dissociation enthalpies were also calculated in the neutral and ionic hydrazine derivatives. In the neutral hydrazines, the loss of a hydrogen atom creates a carbon-centered radical, which is not the case in the ion

$$(CH_3)_2NN(CH_3)_2 \rightarrow (CH_3)_2NNCH_2^{\bullet}(CH_3) + H^{\bullet} \quad (11)$$

$$(CH_3)_2NN(CH_3)_2^{+\bullet} \rightarrow (CH_3)_2NN^{+}{=}CH_2(CH_3) + H^{\bullet} \quad (12)$$

We calculated the DH(H_2C−H) in all three neutral hydrazines to be ∼381 and ∼216 kJ mol^{-1} in the ions. The bond dissociation enthalpies in the neutrals and ions stay constant as the methyl substitution increases. No extra methyl stabilization is expected in the fragment ions compared to the parent radical cation because the charge is still solely located on one of the two nitrogen atoms.

Summary

The lowest energy dissociation channels of methylhydrazine and tetramethylhydrazine ions have been investigated using TPEPICO spectroscopy, tandem mass spectrometry, and VTST. The methylhydrazine ion dissociates by losing a hydrogen atom to form fragment ion *m/z* 45, $CH_2NHNH_2^{+}$, a methyl group to form fragment ion *m/z* 31, $NHNH_2^{+}$, and by rearranging to lose methane and form fragment ion *m/z* 30, $N_2H_2^{+\bullet}$. The tetramethylhydrazine ion dissociates by losing a methyl radical to form fragment ion *m/z* 73, $(CH_3)_2NNCH_3^{+}$, and by losing methane to form fragment ion *m/z* 72, $C_3H_8N_2^{+\bullet}$. VTST was used to locate the transition states of the unimolecular dissociation

TABLE 7: Proton Affinities of N_2H_2, N_2H_4, CH_4N_2, CH_3NHNH_2, $(CH_3)_2NNH_2$, and $(CH_3)_2NN(CH_3)_2$

		Δ_fH(M) (kJ mol^{-1})		PA(M) (kJ mol^{-1})		
neutral molecule (M)	protonated molecule (MH^+)	reported	mG3[a]	experimental[b]	mG3[a]	reported
trans-N_2H_2	$N_2H_3^+$	207.5[34], 208.8[2]	212	777 ± 5, 778 ± 5	768	764 ± 8[3], 803[4c], 782[4d]
cis-N_2H_2	$N_2H_3^+$	227.6[34], 229.7[2]	234	797 ± 5, 799 ± 5	789	
iso-NNH_2	$N_2H_3^+$	321.3[34]	312	890 ± 5	867	
CH_3NNH	$CH_3N\mathbf{N}H_2^+$	196.2[2], 187 ± 12[3], 188 ± 8[3]	197	818 ± 6[2], 809 ± 13[3], 810 ± 10[3]	818	845[4,28], 813 ± 12[3]
	$CH_3\mathbf{N}HNH^+$[e]				815	841[4,28]
$CH_2{=}NNH_2$	$CH_2\mathbf{N}HNH_2^+$	183.0[35], 188.1[35]	189	851 ± 15, 856 ± 15	857	
	$CH_2N\mathbf{N}H_3^+$[e]				838	
	$\mathbf{C}H_3NNH_2^+$				809	
N_2H_4	$N_2H_5^+$[e]		121		859	864.5[36f], 862[36g], 856[36h], 858[28]
CH_3NHNH_2	$CH_3\mathbf{N}H_2NH_2^+$		128		897	895.8[26], 896[28]
	$CH_3NH\mathbf{N}H_3^+$				877	
$(CH_3)_2NNH_2$	$(CH_3)_2\mathbf{N}HNH_2^+$		122		919	918.4[26], 909.2[37i], 921.7[37j], 920.1[37k], 927.1[28]
	$(CH_3)_2NN\mathbf{N}H_3^+$				888	882.8[37i], 887.4[37j]
$(CH_3)_2NN(CH_3)_2$	$(CH_3)_2\mathbf{N}HN(CH_3)_2^+$		135		940	940.6[26], 938.9[38k], 948.7[28]

[a] Present work. [b]PA values determined using the $\Delta_fH_0(MH^+)$ obtained from the VTST fit with $\Delta_fH_0(H^+)^2 = 1528.1$ kJ mol^{-1} and the respective Δ_fH(M) (i.e., $N_2H_2 + H^+ \rightarrow N_2H_3^+$ with $\Delta_fH(N_2H_2) = 207.5$ kJ mol^{-1} taken from Pople and Curtiss[34] gives a PA(trans-N_2H_2) = 777 ± 5 kJ mol^{-1}).[38] [c]PA calculated from SDCI + Pople/6-31G**//6-31G**.[4] [d]PA calculated using the CASSCF-Multireference CI procedure.[4] [e]mG3 $\Delta_fH_0(CH_3NHNH^+) = 914$ kJ mol^{-1}, mG3 $\Delta_fH_0(CH_2NNH_3^+) = 883$ kJ mol^{-1}, and mG3 $\Delta_fH_0(N_2H_5^+) = 793$ kJ mol^{-1} from present work. [f]Calculated from the isodesmic reaction 3 in Armstrong et al.[36] [g]G2(MP2) calculated PA value.[36] [h]Experimental value. [i]PA calculated using M(I) method.[37] [j]PA calculated using M(II) method.[37] [k]PA calculated at 550 K.

TABLE 8: N−C and H−C Bond Dissociation Enthalpies (in kJ Mol^{-1}) in the Neutral and Ionized Hydrazine Derivatives

	$DH_0(N-CH_3)$			$DH_0(H_2C-H)$		
	neutral	ion		neutral	ion	
	mG3	VTST	mG3	mG3	VTST	mG3
methylhydrazine[a]	262	244	262	380	214	216
1,1-dimethylhydrazine[b]	262	225	230	383	207	211
tetramethylhydrazine[c]	257	174	170	381		220

[a] G2 $\Delta_fH_0(NHNH_2^{\bullet}) = 240.7$ kJ mol^{-1} taken from Catoire et al.,[35] mG3 $\Delta_fH_0(CH_2NHNH_2^{\bullet}) = 292$ kJ mol^{-1}, present work. [b]mG3 $\Delta_fH_0(CH_3NNH_2^{\bullet}) = 234$ kJ mol^{-1} and mG3 $\Delta_fH_0((CH_3)(CH_2)NNH_2^{\bullet}) = 289$ kJ mol^{-1}, present work. [c]mG3 $\Delta_fH_0((CH_3)_2NNCH_3^{\bullet}) = 243$ kJ mol^{-1}, mG3 $\Delta_fH_0((CH_3)_2NN(CH_3)(CH_2)^{\bullet}) = 299$ kJ mol^{-1}, and mG3 $\Delta_fH_0((CH_3)_2NN(CH_3)(CH_2)^+) = 813$ kJ mol^{-1}, present work.

reactions (methyl and hydrogen losses) that were then used to reproduce the TPEPICO breakdown diagrams. The transition states of the rearrangement processes (methane loss) were estimated in the fitting procedure. Only small adjustments were needed to fit the experimental results. Enthalpies of formation of fragment ions (*m*/*z* 73, *m*/*z* 72, *m*/*z* 45, *m*/*z* 31, and *m*/*z* 30) were determined from the VTST fits to the TPEPICO data and compared with those from mG3 calculations. Excellent agreement was found for all fragment ions except for fragment ion *m*/*z* 31, $NHNH_2^+$, for which the VTST derived enthalpy of formation was lower than the mG3 calculated one. Two plausible structures of fragment ion *m*/*z* 72 have been proposed (i.e., isomers VI and VII). The breakdown diagrams of MH and TMH ions were recorded from threshold to ~32 eV. Eighteen and twenty-five fragment ions, respectively, have thus been observed, and their AEs are reported. From the derived and calculated Δ_fH_0 of the fragment ions, PAs of small neutral molecules (N_2H_2 and CH_4N_2) were determined as well as the N−C and H−C bond dissociation enthalpies in the three hydrazine derivatives.

Acknowledgment. The authors are grateful to the Council for the Central Laboratory of the Research Councils (U.K.) for the allocation of beamtime at the Daresbury Laboratory Synchrotron Radiation Source. P.M.M. thanks the Natural Sciences and Engineering Research Council of Canada for continuing financial support and the University of Ottawa for seed funds to undertake these experiments. A.-M.B. thanks the Natural Sciences and Engineering Research Council of Canada and the University of Ottawa for scholarships.

Supporting Information Available: This information is available free of charge via the Internet at http://pubs.acs.org.

References and Notes

(1) Burgers, P. C.; Drewello, T.; Schwarz, H.; Terlouw, J. K. *Int. J. Mass Spectrom. Ion Proc.* **1989**, *95*, 157.

(2) Matus, M. H.; Arduengo, A. J. I.; Dixon, D. A. *J. Phys. Chem. A* **2006**, *110*, 10116.

(3) Nguyen, M. T. *Int. J. Mass Spectrom. Ion Proc.* **1994**, *136*, 45.

(4) van Garderen, H. F.; Ruttink, P. J. A.; Burgers, P. C.; McGibbon, G. A.; Terlouw, J. K. *Int. J. Mass Spectrom. Ion Proc.* **1992**, *121*, 159.

(5) Kimura, K.; Katsumata, S.; Achiba, Y.; Yamazaki, T.; Iwata, S. *Handbook of HeI Photoelectron Spectra of Fundamental Organic Molecules*; Japan Scientific Societies Press: Tokyo, 1981.

(6) Houk, K. N. *J. Am. Chem. Soc.* **1975**, *97*, 1824.

(7) Boyd, R. J.; Bunzli, J. C.; Snyder, J. P.; Heyman, M. L. *J. Am. Chem. Soc.* **1973**, *95*, 6478.

(8) Dibeler, V. H.; Franklin, J. L.; Reese, R. M. *J. Am. Chem. Soc.* **1959**, *81*, 68.

(9) Harshman, R. C. *Jet Propul.* **1957**, *27*, 398.

(10) Franklin, J. L. *Ind. Eng. Chem.* **1949**, *41*, 1070.

(11) Boulanger, A.-M.; Rennie, E. E.; Holland, D. M. P.; Shaw, D. A.; Mayer, P. M. *J. Phys. Chem. A* **2006**, *110*, 8563.

(12) Holmes, J. L.; Aubry, C.; Mayer, P. M. *Assigning structures to ions in mass spectrometry*; CRC Press: Boca Raton, 2007.

(13) Cooks, R. G.; Beynon, J. H.; Caprioli, R. M.; Lester, G. R. *Metastable Ions*; Elsevier: Amsterdam, 1973.

(14) Boulanger, A.-M.; Rennie, E. E.; Holland, D. M. P.; Shaw, D. A.; Mayer, P. M. *J. Chem. Phys. A* **2007**, *111*, 10884.

(15) Boulanger, A.-M.; Rennie, E. E.; Holland, D. M. P.; Shaw, D. A.; Mayer, P. M. *J. Phys. Chem. A* **2007**, *111*, 5388.

(16) Holland, D. M. P.; Shaw, D. A.; Sumner, I.; Hayes, M. A.; Mackie, R. A.; Wannberg, B.; Shpinkova, L. G.; Rennie, E. E.; Cooper, L.; Johnson, C. A. F.; Parker, J. E. *Nucl. Instr. Methods Phys. Res., Sect. B* **2001**, *179*, 436.

(17) Holland, D. M. P.; West, J. B.; Macdowell, A. A.; Munro, I. H.; Beckett, A. G. *Nucl. Instr. Methods Phys. Res., Sect. B* **1989**, *44*, 233.

(18) Rennie, E. E.; Cooper, L.; Johnson, C. A. F.; Parker, J. E.; Mackie, R. A.; Shpinkova, L. G.; Holland, D. M. P.; Shaw, D. A.; Hayes, M. A. *Chem. Phys.* **2001**, *263*, 149.

(19) Holmes, J. L.; Mayer, P. M. *J. Phys. Chem.* **1995**, *99*, 1366.

(20) Frisch, M. J.; Trucks, G. W.; Schlegel, H. B.; Scuseria, G. E.; Robb, M. A.; Cheeseman, J. R.; Zakrzewski, V. G.; Montgomery, J. A.; Stratmann, R. E.; Burant, J. C.; Dapprich, S.; Millam, J. M.; Daniels, A. D.; Kudin, K. N.; Strain, M. C.; Farkas, O.; Tomasi, J.; Barone, V.; Cossi, M.; Cammi, R.; Mennucci, B.; Pomelli, C.; Adamo, C.; Clifford, S.; Ochterski, J.; Petersson, G. A.; Ayala, P. Y.; Cui, Q.; Morokuma, K.; Malick, D. K.; Rabuck, A. D.; Raghavachari, K.; Foresman, J. B.; Cioslowski, J.; Ortiz, J. V.; Stefanov, B. B.; Liu, G.; Liashenko, A.; Piskorz, P.; Komaromi, I.; Gomperts, R.; Martin, R. L.; Fox, D. J.; Keith, T.; Al-Laham, M. A.; Peng, C. Y.; Nanayakkara, A.; Gonzalez, C.; Challacombe, M.; Gill, P. M. W.; Johnson, B.; Chen, W.; Wong, M. W.; Andres, J. L.; Gonzalez, C.; Head-Gordon, M.; Replogle, E. S.; Pople, J. A. *GAUSSIAN 98*, revision A.6; Gaussian Inc.: Pittsburgh PA, 1998.

(21) Curtiss, L. A.; Raghavachari, K.; Redfern, P. C.; Rassolov, V.; Pople, J. A. *J. Chem. Phys.* **1998**, *109*, 7764.

(22) Nicolaides, A.; Rauk, A.; Glukhovtsev, M. N.; Radom, L. *J. Phys. Chem.* **1996**, *100*, 17460.

(23) Baer, T.; Hase, W. L. *Unimolecular Reaction Dynamics, Theory and Experiments*; Oxford University Press: New York, 1996.

(24) East, A. L. L.; Radom, L. *J. Chem. Phys.* **1997**, *106*, 6655.

(25) *NIST Chemistry WebBook*, NIST Standard Reference Database Number 69; Mallard, W. G.; Linstrom, P. J., Eds.; National Institute of Standards and Technology: Gaithersburg, MD, 2000; Vol. (http://webbook.nist.gov).

(26) Meot-Ner, M.; Nelsen, S. F.; Willi, M. R.; Frigo, T. B. *J. Am. Chem. Soc.* **1984**, *106*, 7384.

(27) Holmes, J. L. The Correlation of Thermochemical Data. In *The Encyclopedia of Mass Spectrometry*; Gross, M. L., Ed.; Elsevier Inc.: San Diego, CA, 2003; Vol. 1, pp 434.

(28) Hunter, E. P.; Lias, S. G. *J. Phys. Chem. Ref. Data* **1998**, *27*, 413.

(29) Blanskby, S. J.; Ellison, G. B. *Acc. Chem. Res.* **2003**, *36*, 255.

(30) Foner, S. N.; Hudson, R. L. *J. Chem. Phys.* **1970**, *53*, 4377.

(31) Akopyan, M. E.; Vilesov, F. I. *Kinet. Katal.* **1963**, *4*, 39.

(32) Syage, J. A. *J. Chem. Phys.* **1992**, *97*, 6085.

(33) Gowenlock, B. G.; Jones, P. P.; Majer, J. R. *Trans. Faraday Soc.* **1961**, *57*, 23.

(34) Pople, J. A.; Curtiss, L. A. *J. Chem. Phys.* **1991**, *95*, 4385.

(35) Catoire, L.; Swihart, M. T. *J. Propul. Power* **2002**, *18*, 1242.

(36) Armstrong, D. A.; Yu, D.; Rauk, A. *J. Phys. Chem. A* **1997**, *101*, 4761.

(37) Hillebrand, C.; Klessinger, M.; Eckert-Maksic, M.; Maksic, Z. B. *J. Phys. Chem.* **1996**, *100*, 9698.

(38) Nelsen, S. F.; Rumack, D. T.; Sieck, L. W.; Meot-Ner, M. *J. Am. Chem. Soc.* **1988**, *110*, 6303.